

25 **Abstract**

26 Group B *Streptococcus* (GBS) is a major human pathogen, causing meningitis and severe
27 infection in newborns, yet little is known about its lipid membrane. Here, we investigated
28 the GBS lipid membrane and identify a novel cationic glycolipid, lysyl-glucosyl-
29 diacylglycerol (Lys-Glc-DAG). Multiple peptide resistance factor (MprF) is highly
30 conserved in many bacterial pathogens and plays a critical role in resistance against
31 cationic antimicrobial peptides, cationic bacteriocins, and antibiotics. The MprF protein
32 has been shown to catalyze the amino-acylation of the anionic phospholipid
33 phosphatidylglycerol (PG). Most notably, MprF uses L-lysyl-tRNA to esterify PG with a
34 positively charged lysine to produce lysyl-phosphatidylglycerol (Lys-PG). We
35 demonstrate through heterologous host expression and gene deletion that the GBS MprF
36 has an expanded substrate repertoire and is the biosynthetic enzyme responsible for both
37 Lys-Glc-DAG and Lys-PG biosynthesis in GBS. Furthermore, we demonstrate that MprF
38 contributes specifically to meningitis pathogenesis at the blood-brain barrier both *in vitro*
39 and in an *in vivo* hematogenous murine infection model but does not contribute to
40 bloodstream survival. These results greatly expand our knowledge of MprF functions and
41 reveal insights into the survival mechanisms and pathogenesis of meningitis caused by
42 GBS.

43

44 **Importance**

45 The lipidomes of many important Gram-positive human pathogens remain largely
46 uncharacterized. By investigating the lipid membrane of *Streptococcus agalactiae* (Group
47 B *Streptococcus*; GBS), an etiological agent responsible for meningitis and severe

48 diseases in newborns, we uncovered a novel glycolipid and biochemical activity of
49 Multiple peptide resistance factor (MprF) in GBS. MprF is known to add lysine to
50 phosphatidylglycerol (PG), forming Lys-PG. We show in GBS that it also adds lysine to
51 the glycolipid, glucosyl-diacylglycerol (Glc-DAG), to form Lys-Glc-DAG. We demonstrate
52 the GBS MprF contributes to brain entry and meningitis pathogenesis in mice. These
53 results expand our knowledge of MprF functions and reveal insights into the survival
54 mechanisms and pathogenesis of meningitis caused by GBS.

55

56 **Observation**

57 *Streptococcus agalactiae* (Group B *Streptococcus*; GBS) is a Gram-positive bacterium
58 that colonizes the lower genital and gastrointestinal tracts of ~30% of healthy women (1,
59 2). GBS causes sepsis and pneumonia in neonates and is a leading cause of neonatal
60 meningitis, resulting in long-lasting neurological effects in survivors (3-5). New therapeutic
61 and preventative approaches and a more complete understanding of GBS pathogenesis
62 are needed to mitigate the devastating impact of GBS on neonates. Despite the critical
63 role of the bacterial membrane in host-pathogen interactions, little is known about this for
64 GBS. Here, we investigated GBS membrane lipids using normal phase liquid
65 chromatography (NPLC) coupled with electrospray ionization (ESI) high-resolution
66 tandem mass spectrometry (HRMS/MS).

67

68 **GBS lipidomic profile**

69 The membrane lipids of three GBS clinical isolates of representative serotypes were
70 characterized: COH1 (6), A909 (7), and CNCTC 10/84 (serotypes III, 1a, and V,
71 respectively) (8). Common Gram-positive bacterial lipids were identified by normal phase
72 LC coupled with negative ion ESI/MS/MS, including diacylglycerol (DAG),
73 monohexosyldiacylglycerol (MHDAG), dihexosyldiacylglycerol (DHDAG),
74 phosphatidylglycerol (PG), and lysyl-phosphatidylglycerol (Lys-PG), as shown by the
75 negative total ion chromatogram (TIC) (Fig. 1A).

76

77 Surprisingly, the positive TIC (Fig. 1B, Supplemental Figure S1) shows highly abundant
78 peaks of unknown identity at the retention time ~25-29 min. The mass spectra (Fig. 1C)
79 and LC retention times of this lipid do not match with any other bacterial lipids we have

80 analyzed or exact masses in lipidomic databases. Tandem MS (MS/MS) in the positive
81 ion mode (Fig. 1D), negative ion mode (Fig. 1E), and high-resolution mass measurement
82 (Fig. 1C) allowed us to propose lysyl-glucosyl-diacylglycerol (Lys-Glc-DAG) (Fig. 1F) as
83 the structure of this unknown lipid. Observed and exact masses of Lys-Glc-DAG are
84 shown in Table S1. The assignment of glucose was based on the observation that
85 glucosyl-diacylglycerol (Glc-DAG) is a major membrane component of GBS and other
86 streptococci (9), and results from an isotopic labeling experiment using ^{13}C -labeled
87 glucose (Glucose- $^{13}\text{C}_6$). The assignment of lysine modification was supported by an
88 isotopic labeling experiment with deuterated lysine (lysine- d_4). The expected mass shifts
89 (+4 Da) were observed in both molecular ions and MS/MS product ions (Supplemental
90 Figure S2). Comparison of both MS/MS spectra of labeled (Glucose- $^{13}\text{C}_6$) and unlabeled
91 Lys-Glc-DAG indicates the lysine residue is linked to the 6-position of glucose
92 (Supplemental Figure S2). Lys-Glc-DAG consists of several molecular species with
93 different fatty acyl compositions resulting in different retention times and multiple,
94 unresolved TIC peaks (~25-29 min).

95

96 **GBS MprF synthesizes Lys-PG and Lys-Glc-DAG**

97 The enzyme MprF (multiple peptide resistance factor) catalyzes the aminoacylation of PG
98 with lysine in some Gram-positive pathogens (10, 11). GBS MprF is responsible and
99 sufficient for synthesizing both Lys-Glc-DAG and Lys-PG. Deletion of *mprF* from COH1
100 abolishes both Lys-Glc-DAG and Lys-PG synthesis, which are restored by
101 complementation (Fig. 1G). Deletion of GBS *mprF* does not confer a growth defect in
102 Todd-Hewitt broth or tissue culture medium. The oral colonizer *Streptococcus mitis* does

103 not encode *mprF* or synthesize Lys-PG, but synthesizes Glc-DAG and PG (12, 13).
104 Heterologous expression of GBS *mprF* in *S. mitis* results in Lys-Glc-DAG and Lys-PG
105 production (Fig. 1H), while expression of *Enterococcus faecium mprF* results in only Lys-
106 PG production (Fig. 1H), as expected (14). Biosynthetic pathways involving MprF are
107 shown in Fig. 1I.

108

109 **MprF contributes to GBS pathogenesis**

110 We investigated whether MprF contributes to GBS invasion into brain endothelial cells
111 and development of meningitis. To mimic the human blood-brain barrier (BBB), we utilized
112 the human cerebral microvascular endothelial cell line hCMEC/D3. *In vitro* assays for
113 adhesion and invasion were performed as described previously (9, 15, 16). There was no
114 significant difference in the ability of $\Delta mprF$ compared to WT and complement cells to
115 attach to hCMEC/D3 cells (Fig. 2A). However, we observed a significant decrease in the
116 amount of $\Delta mprF$ recovered from the intracellular compartment of hCMEC/D3 cells (Fig.
117 2A). The reduced invasion phenotype was confirmed in the hypervirulent serotype V
118 strain, CJB111 (17, 18) (Supplemental Figure S3). Intracellular survival requires GBS to
119 survive low pH conditions in lysosomes (pH 4.5 – 5.5) (19), and $\Delta mprF$ is unable to survive
120 low pH conditions (Fig. 2B). This suggests that MprF promotes GBS invasion into the
121 BBB, and intracellular survival.

122

123 We hypothesized that these *in vitro* phenotypes of $\Delta mprF$ would translate into a
124 diminished ability to penetrate the BBB and produce meningitis *in vivo*. Using our

125 standard model of GBS hematogenous meningitis (9, 15) mice were challenged with
126 either WT GBS or $\Delta mprF$. Mice were sacrificed at 72 h to determine bacterial loads in
127 blood and brain tissue. We recovered significantly less CFU in the brains of $\Delta mprF$ -
128 infected mice compared to the WT-infected mice (Fig. 2C). However, there was no
129 significant difference in CFU recovered from the bloodstream (Fig. 2D), demonstrating
130 that $\Delta mprF$ does not have a general *in vivo* growth defect. Furthermore, mice challenged
131 with WT GBS had significantly more leukocyte infiltration, meningeal thickening and
132 neutrophil chemokine, KC, in brain homogenates compared to $\Delta mprF$ mutant-infected
133 animals (Fig. 2E-G). Taken together, *mprF* contributes to GBS penetration into the brain
134 and to the pathogenesis of meningitis *in vivo*.

135

136 **Conclusion**

137 Bacteria use enzymes such as MprF to fine-tune cell envelope properties for stress
138 response and virulence. We discovered that GBS MprF uniquely synthesizes a novel and
139 highly abundant cationic glycolipid, Lys-Glc-DAG, as well as Lys-PG. This establishes
140 that GBS capitalizes on MprF to modulate charges of both glycolipids and phospholipids
141 at the membrane. Deletion of *mprF* impacts GBS virulence. Interestingly, this effect is
142 observed for meningitis, and not for bacteremia, demonstrating that MprF and/or MprF-
143 synthesized lipids play specific roles in BBB penetration but not *in vivo* survival in general.
144 In future studies, generating GBS MprF variants that synthesize only Lys-Glc-DAG or
145 Lys-PG at wild-type levels will allow for identification of the specific roles each lipid plays
146 in meningitis.

147

148 Our identification of the novel Lys-Glc-DAG glycolipid rationalizes further study of the
149 lipidomes of human pathogens. The decreased *in vivo* pathogenicity of $\Delta mprF$ identifies
150 GBS MprF as a candidate for targeting by antimicrobial strategies. Moreover, that Lys-
151 Glc-DAG is a major GBS membrane component holds promise that Lys-Glc-DAG could
152 be utilized as a specific molecular biomarker for GBS diagnostics.

153

154 **Materials and methods**

155 Methods were performed using established techniques; see Supplemental Text S1.
156 Strains listed in Table S2 and primers Table S3. Illumina sequence reads are deposited
157 in the Sequence Read Archive, accession PRJNA675025.

158

159 **Conflict of interest**

160 The authors have declared that no conflict of interest exists.

161

162 **Acknowledgements**

163 We thank Kathryn Patras at the University of California San Diego for the CNCTC 10/84
164 strain and Moutusee Islam in Kelli Palmer's lab at The University of Texas at Dallas for
165 *E. faecium* 1,231,410 DNA.

166

167 The work was supported in part by T32 5T32AI052066-18 for H.S.M, the Coordenação
168 de Aperfeiçoamento de Pessoal de Nível Superior, Brazil (CAPES; finance code 001 to
169 J.D.C.M), by grant R01NS116716 from the National Institutes of Health (NIH) to K.S.D
170 and associated supplement from NINDS to R.V, NIH grant R21AI130666 and the Cecil

171 H. and Ida Green Chair in Systems Biology Science to K.P, NIH grant R56AI139105 to
172 K.P and Z.G, and NIH grant U54GM069338 to Z.G.

173

174 **References**

- 175 1. Wilkinson HW. 1978. Group B Streptococcal Infection in Humans. Annual Review
176 of Microbiology 32:41-57.
- 177 2. Doran KS, Nizet V. 2004. Molecular pathogenesis of neonatal Group B
178 Streptococcal infection: No longer in its infancy. Molecular Microbiology 54:23-
179 31.
- 180 3. Hall J, Adams NH, Bartlett L, Seale AC, Lamagni T, Bianchi-Jassir F, Lawn JE,
181 Baker CJ, Cutland C, Heath PT, Ip M, Le Doare K, Madhi SA, Rubens CE, Saha
182 SK, Schrag S, Sobanjo-Ter Meulen A, Vekemans J, Gravett MG. 2017. Maternal
183 Disease With Group B *Streptococcus* and Serotype Distribution Worldwide:
184 Systematic Review and Meta-analyses. Clinical Infectious Diseases 65:S112-
185 S124.
- 186 4. Schuchat A. 1998. Epidemiology of Group B Streptococcal disease in the United
187 States: shifting paradigms. Clinical Microbiology Reviews 11:497-513.
- 188 5. Edwards MS, Rench MA, Haffar AA, Murphy MA, Desmond MM, Baker CJ. 1985.
189 Long-term sequelae of Group B Streptococcal meningitis in infants. The Journal
190 of Pediatrics 106:717-22.
- 191 6. Kuypers JM, Heggen LM, Rubens CE. 1989. Molecular analysis of a region of
192 the Group B *Streptococcus* chromosome involved in type III capsule expression.
193 Infection and Immunity 57:3058-65.
- 194 7. Lancefield RC, McCarty M, Everly WN. 1975. Multiple mouse-protective
195 antibodies directed against Group B Streptococci. Special reference to antibodies
196 effective against protein antigens. The Journal of Experimental Medicine
197 142:165-79.
- 198 8. Wilkinson HW. 1977. Nontypable Group B Streptococci isolated from human
199 sources. Journal of Clinical Microbiology 6:183-4.
- 200 9. Doran KS, Engelson EJ, Khosravi A, Maisey HC, Fedtke I, Equils O, Michelsen
201 KS, Arditi M, Peschel A, Nizet V. 2005. Blood-brain barrier invasion by Group B
202 *Streptococcus* depends upon proper cell-surface anchoring of lipoteichoic acid.
203 The Journal of Clinical Investigation 115:2499-507.
- 204 10. Peschel A, Jack RW, Otto M, Collins LV, Staubitz P, Nicholson G, Kalbacher H,
205 Nieuwenhuizen WF, Jung G, Tarkowski A, Van Kessel KPM, Van Strijp JAG.
206 2001. *Staphylococcus aureus* resistance to human defensins and evasion of
207 neutrophil killing via the novel virulence factor MprF is based on modification of
208 membrane lipids with L-lysine. Journal of Experimental Medicine 193:1067-1076.
- 209 11. Roy H, Ibba M. 2008. RNA-dependent lipid remodeling by bacterial multiple
210 peptide resistance factors. Proceedings of the National Academy of Sciences of
211 the United States of America 105:4667-4672.

- 212 12. Joyce LR, Guan Z, Palmer KL. 2019. Phosphatidylcholine Biosynthesis in Mitis
213 Group Streptococci via Host Metabolite Scavenging. *Journal of Bacteriology*
214 201:e00495-19.
- 215 13. Adams HM, Joyce LR, Guan Z, Akins RL, Palmer KL. 2017. *Streptococcus mitis*
216 and *S. oralis* Lack a Requirement for CdsA, the Enzyme Required for Synthesis
217 of Major Membrane Phospholipids in Bacteria. *Antimicrobial Agents and*
218 *Chemotherapy* 61:e02552-16.
- 219 14. Roy H. 2009. Tuning the properties of the bacterial membrane with
220 aminoacylated phosphatidylglycerol. *IUBMB Life* 61:940-953.
- 221 15. Deng L, Spencer BL, Holmes JA, Mu R, Rego S, Weston TA, Hu Y, Sanches GF,
222 Yoon S, Park N, Nagao PE, Jenkinson HF, Thornton JA, Seo KS, Nobbs AH,
223 Doran KS. 2019. The Group B Streptococcal surface antigen I/II protein, BspC,
224 interacts with host vimentin to promote adherence to brain endothelium and
225 inflammation during the pathogenesis of meningitis. *PLoS Pathogens*
226 15:e1007848.
- 227 16. Spencer BL, Deng L, Patras KA, Burcham ZM, Sanches GF, Nagao PE, Doran
228 KS. 2019. Cas9 contributes to Group B Streptococcal colonization and disease.
229 *Frontiers in Microbiology* 10:1-15.
- 230 17. Faralla C, Metruccio MM, De Chiara M, Mu R, Patras KA, Muzzi A, Grandi G,
231 Margarit I, Doran KS, Janulczyk R. 2014. Analysis of two-component systems in
232 group B *Streptococcus* shows that RgfAC and the novel FspSR modulate
233 virulence and bacterial fitness. *mBio* 5:e00870-14.
- 234 18. Spencer BL, Chatterjee A, Duerkop BA, Baker CJ, Doran KS. 2021. Complete
235 Genome Sequence of Neonatal Clinical Group B Streptococcal Isolate CJB111.
236 *Microbiology Resource Announcements* 10.
- 237 19. Mu R, Cutting AS, Del Rosario Y, Villarino N, Stewart L, Weston TA, Patras KA,
238 Doran KS. 2016. Identification of CiaR Regulated Genes That Promote Group B
239 Streptococcal Virulence and Interaction with Brain Endothelial Cells. *PLoS One*
240 11:e0153891.

241

242

243 **Figure legends**

244 **Fig 1.** Total ion chromatogram (TIC) of LC/MS in A) negative ion mode, B) positive ion
245 mode shows a major unknown lipid eluting at ~25-29 min. C) Positive ESI/MS showing
246 the $[M+H]^+$ ions of the unknown lipid. D) Positive ion MS/MS spectrum of $[M+H]^+$ at m/z
247 885.6 and E) negative ion MS/MS spectrum of $[M-H]^-$ at m/z 883.6 of the unknown lipid.
248 F) Lys-Glc-DAG (16:0/18:1) is proposed as the structure of the unknown lipid. G) TIC
249 showing loss of Lys-Glc-DAG and Lys-PG in COH1 $\Delta mprF$ which is present when *mprF*
250 is complemented *in trans*. H) Lys-Glc-DAG and Lys-PG is only present in *S. mitis* when
251 expressing GBS *mprF* compared to Lys-PG only when expressing *E. faecium mprF*. “*”
252 denotes methylcarbamate of Lys-Glc-DAG, an extraction artifact due to the use of
253 chloroform. I) Biosynthetic pathways involving MprF.

254 **Fig 2.** A) *In vitro* assays for adherence and invasion of hCMEC cells indicates *mprF*
255 contributes to invasion but not adherence to brain endothelium (mean of 3 replicate
256 experiments with 4 technical replicates, mean and SEM). B) pH-adjusted medium growth
257 indicates $\Delta mprF$ cannot survive in low pH conditions, mean and SD. Groups of CD-1 mice
258 were injected intravenously with COH1 WT or COH1 $\Delta mprF$ strains and bacterial counts
259 were assessed in the C) brain and D) blood after 72h. Representative data from 2
260 independent experiments are shown (WT, $n = 20$; $\Delta mprF$, $n = 19$). E) Hematoxylin-eosin-
261 stained brain sections from representative mice infected with WT (top) or $\Delta mprF$ mutant
262 (bottom); arrows indicate meningeal thickening and leukocyte infiltration. F) Quantification
263 of meningeal thickening using ImageJ. G) KC chemokine production measured by ELISA.
264 Panels C,D,F, and G) median indicated. Statistical analyses performed using GraphPad
265 Prism: A) One-way ANOVA with Tukey’s multiple comparisons test; C,D,F) unpaired two-
266 tailed t-test; G) Mann-Whitney U test; p-values indicated; ns, no significance (p-value >
267 0.05).

268

269 **Supplemental files**

270 Supplemental Text S1: Materials and Methods

271 Supplemental Figure S1. Detection of Lys-PG and Lys-Glc-DAG in *S. agalactiae* A909
272 and *S. agalactiae* CNCTC 10/84.

273 Supplemental Figure S2. Isotopic incorporation of deuterated lysine and ^{13}C -labeled
274 glucose into Lys-Glc-DAG and Lys-PG.

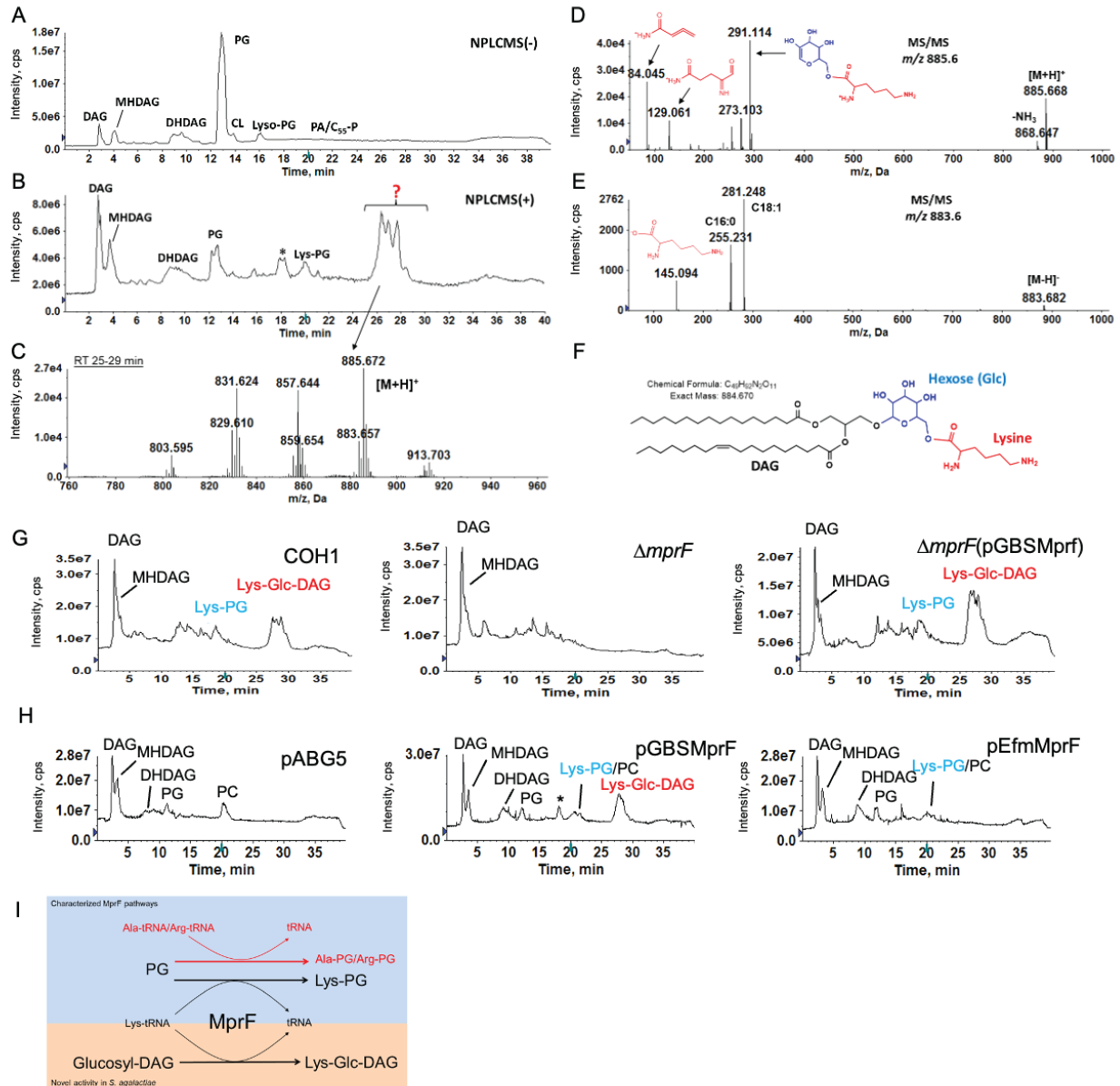
275 Supplemental Figure S3. *In vitro* hCMEC adhesion and invasion of CJB111 strains.

276 Supplemental Table S1. Observed and calculated exact masses of the $[M+H]^+$ ions of
277 Lys-Glc-DAG molecular species in *S. agalactiae* COH1.

278 Supplemental Table S2. Strains and plasmids used in this study.

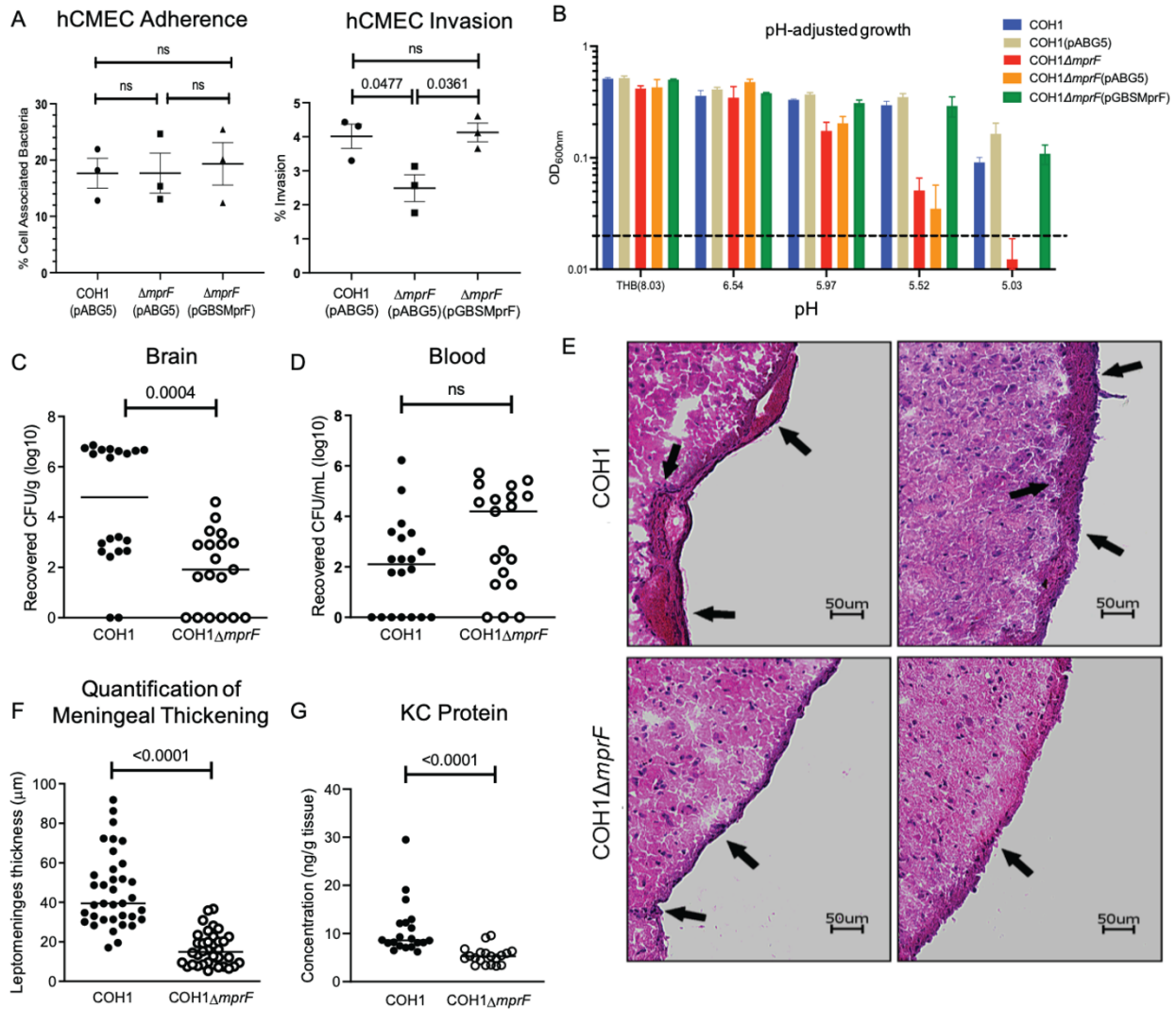
279 Supplemental Table S3. Primers used in this study.

280



281

282 **Fig 1.** Total ion chromatogram (TIC) of LC/MS in A) negative ion mode, B) positive ion
 283 mode shows a major unknown lipid eluting at ~25-29 min. C) Positive ESI/MS showing
 284 the $[M+H]^+$ ions of the unknown lipid. D) Positive ion MS/MS spectrum of $[M+H]^+$ at m/z
 285 885.6 and E) negative ion MS/MS spectrum of $[M-H]^-$ at m/z 883.6 of the unknown lipid.
 286 F) Lys-Glc-DAG (16:0/18:1) is proposed as the structure of the unknown lipid. G) TIC
 287 showing loss of Lys-Glc-DAG and Lys-PG in COH1 $\Delta mprF$ which is present when *mprF* is
 288 complemented *in trans*. H) Lys-Glc-DAG and Lys-PG is only present in *S. mitis* when
 289 expressing GBS *mprF* compared to Lys-PG only when expressing *E. faecium mprF*. “*”
 290 denotes methylcarbamate of Lys-Glc-DAG, an extraction artifact due to the use of
 291 chloroform. I) Biosynthetic pathways involving MprF.



292

293 **Fig 2.** A) *In vitro* assays for adherence and invasion of hCMEC cells indicates *mprF*
 294 contributes to invasion but not adherence to brain endothelium (mean of 3 replicate
 295 experiments with 4 technical replicates, mean and SEM). B) pH-adjusted medium growth
 296 indicates $\Delta mprF$ cannot survive in low pH conditions, mean and SD. Groups of CD-1 mice
 297 were injected intravenously with COH1 WT or COH1 $\Delta mprF$ strains and bacterial counts
 298 were assessed in the C) brain and D) blood after 72h. Representative data from 2
 299 independent experiments are shown (WT, $n = 20$; $\Delta mprF$, $n = 19$). E) Hematoxylin-eosin-
 300 stained brain sections from representative mice infected with WT (top) or $\Delta mprF$ mutant
 301 (bottom); arrows indicate meningeal thickening and leukocyte infiltration. F) Quantification
 302 of meningeal thickening using ImageJ. G) KC chemokine production measured by ELISA.
 303 Panels C,D,F, and G) median indicated. Statistical analyses performed using GraphPad
 304 Prism: A) One-way ANOVA with Tukey's multiple comparisons test; C,D,F) unpaired two-
 305 tailed t-test; G) Mann-Whitney U test; p-values indicated; ns, no significance (p-value >
 306 0.05).

307
308
309
310
311
312
313
314
315
316
317
318
319
320
321
322

Supplemental Text, Figures, and Tables

***Streptococcus agalactiae* MprF synthesizes a novel cationic glycolipid and contributes to brain entry and meningitis**

Luke R. Joyce^a, Haider S. Manzer^b, Jéssica da C. Mendonça^b, Ricardo Villarreal^b, Kelly S. Doran^{b#}, Kelli L. Palmer^{a#}, and Ziqiang Guan^{c#}

^aDepartment of Biological Sciences, The University of Texas at Dallas, Richardson, TX, 75080

^bDepartment of Immunology and Microbiology, University of Colorado School of Medicine, Aurora, CO, 80045

^cDepartment of Biochemistry, Duke University Medical Center, Durham, NC, 27710

[#]Corresponding authors

323 **Supplemental Text S1: Materials and Methods**

324 **Bacterial strains, media, and growth conditions**

325 GBS strains were grown statically at 37°C in Todd-Hewitt Broth (THB) and *S. mitis* strains were
326 grown statically at 37°C and 5% CO₂, unless otherwise stated. Streptococcal chemically defined
327 medium (20) was diluted from stock as described (21) with 1% w/v glucose (referred to as DM),
328 slightly modified from (22), unless otherwise stated. *Escherichia coli* strains were grown in
329 Lysogeny Broth (LB) at 37°C with rotation at 225 rpm. Kanamycin and erythromycin (Sigma-
330 Aldrich) were supplemented to media at 50 µg/mL and 300 µg/mL for *E. coli*, respectively, or 300
331 µg/mL and 5 µg/mL, respectively, for streptococcal strains.

332

333 **Routine molecular biology techniques**

334 All PCR reactions utilized Phusion polymerase (Thermo Fisher). PCR products and restriction
335 digest products were purified using GeneJET PCR purification kit (Thermo Fisher) per
336 manufacturer protocols. See Table S3 for primers. Plasmids were extracted using GeneJET
337 plasmid miniprep kit (Thermo Fisher) per manufacturer protocols. Restriction enzyme digests
338 utilized XbaI, XhoI, and PstI (New England Biolabs) for 3 h at 37°C in a water bath. Ligations
339 utilized T4 DNA ligase (New England Biolabs) at 16°C overnight or Gibson Assembly Master Mix
340 (New England Biolabs) per manufacturer protocols where stated. All plasmid constructs were
341 sequence confirmed by Sanger sequencing (Massachusetts General Hospital DNA Core or CU
342 Anschutz Molecular Biology Core).

343

344

345 **Deuterated lysine and $^{13}\text{C}_6\text{-D-glucose}$ isotope tracking**

346 A GBS COH1 colony was inoculated into 15 mL of DM containing 450 μM lysine-*d4* (Cambridge
347 Isotopes Laboratories) or a single COH1 colony was inoculated into 10 mL DM supplemented
348 with 0.5% w/v $^{13}\text{C}_6\text{-D-glucose}$ (U-13C6, Cambridge Isotopes Laboratories) for overnight growth for
349 lipidomic analysis described below.

350

351 **Construction of MprF expression plasmids**

352 Genomic DNA was isolated using the Qiagen DNeasy Blood and Tissue kit per the manufacturer's
353 protocol with the exception that cells were pre-treated with 180 μL 50 mg/mL lysozyme, 25 μL
354 2500 U/mL mutanolysin, and 15 μL 20 mg/mL pre-boiled RNase A and incubated at 37°C for 2 h.
355 The *mprF* genes from GBS COH1, (GBSCOH1_1931), GBS CJB111 (ID870_10050), and *E.*
356 *faecium* 1,231,410 (EFTG_00601) were amplified and either Gibson ligated into pABG5 Δ *phoZ*
357 (23) or ligated into pDCErm (24). Plasmid constructs were transformed into chemical competent
358 *E. coli*. Briefly, chemically competent cells were incubated for 10 min on ice with 5 μL of Gibson
359 reaction before heat shock at 42°C for 70 sec, then placed on ice for 2 min before 900 μL of cold
360 SOC medium was added. Outgrowth was performed at 37°C, with shaking at 225 rpm, for 1 h.
361 Cultures were plated on LB agar plates containing 50 $\mu\text{g}/\text{mL}$ kanamycin. Colonies were screened
362 by PCR for presence of the *mprF* insert.

363

364 **Expression of *mprF* in *S. mitis***

365 Natural transformation was performed as previously described (12). Briefly, precultures were
366 thawed at room temperature, diluted in 900 μL of THB, further diluted 1:50 in prewarmed 5 mL
367 THB, and incubated for 45 min at 37°C. 500 μL of culture was then aliquoted with 1 μL of 1 mg/ml

368 competence-stimulating peptide (EIRQTHNIFFNFFKRR) and 1 µg/mL plasmid. Transformation
369 reaction mixtures were cultured for 2 h at 37°C in microcentrifuge tubes before being plated on
370 THB agar supplemented with 300 µg/mL kanamycin. Single transformant colonies were cultured
371 in 15 mL THB overnight. PCR was used to confirm the presence of the *mprF* insert on the plasmid.
372 Plasmids were extracted and sequence confirmed as described above. Lipidomics was performed
373 as described below in biological triplicate.

374

375 **Construction of *mprF* deletion plasmid**

376 Regions ~2 kb upstream and downstream of the GBS COH1 *mprF* (GBSCOH1_1931) or CJB111
377 (ID870_10050) were amplified using PCR. Plasmid, pMBSacB (25), and the PCR products were
378 digested using appropriate restriction enzymes and ligated overnight. 7 µL of the ligation reaction
379 was transformed into chemically competent *E. coli* DH5α as described above, except that
380 outgrowth was performed at 28°C with shaking at 225 rpm for 90 min prior to plating on LB agar
381 supplemented with 300 µg/mL erythromycin. Plates were incubated at 28°C for 72 h. Colonies
382 were screened by PCR for correct plasmid construction. Positive colonies were inoculated into 50
383 mL LB media containing antibiotic and incubated at 28°C with rotation at 225 rpm for 72 h.
384 Cultures were pelleted using a Sorvall RC6+ centrifuge at 4,280 x *g* for 6 min at room temperature.
385 Plasmid was extracted as described above except the cell pellet was split into 5 columns to
386 prevent overloading and serial eluted into 50 µL. Plasmid construction was confirmed via
387 restriction digest using XhoI and XbaI, and the insert was PCR amplified and sequence-verified.

388

389

390

391 **Generation of electrocompetent GBS cells for *mprF* knockout**

392 Electrocompetent cells were generated as described (25) with minor modifications. Briefly, a GBS
393 COH1 or CJB111 colony was inoculated in 5 mL M17 medium (BD Bacto) with 0.5% glucose and
394 grown overnight at 37°C. The 5 mL was used to inoculate a second overnight culture of 50 mL
395 pre-warmed filter-sterilized M17 medium containing 0.5% glucose, 0.6% glycine, and 25% PEG
396 8000. The second overnight was added to 130 mL of the same medium and grown for 1 h at
397 37°C. Cells were pelleted at 3,200 x *g* in a Sorvall RC6+ at 4°C for 10 min. Cells were washed
398 twice with 25 mL cold filter-sterilized GBS wash buffer containing 25% PEG 8000 and 10%
399 glycerol in water, and pelleted as above. Cell pellets were re-suspended in 1 mL GBS wash buffer
400 and either used immediately for transformation or stored in 100 µL aliquots at -80°C until use.

401

402 **Deletion of GBS COH1 and CJB111 *mprF***

403 Electrocompetent cells were generated as described (25) with minor modifications. The double
404 crossover homologous recombination knockout strategy was performed as described previously
405 (16, 25, 26) with minor modifications. 1 µg of plasmid was added to electrocompetent GBS cells
406 and transferred to a cold 1 mm cuvette (Fisher or BioRad). Electroporation was carried out at 2.5
407 kV on an Eppendorf eporator. 1 mL of THB containing 12.5% PEG 8000, 20 mM MgCl₂, and 2
408 mM CaCl₂ was immediately added and then the entire reaction was transferred to a glass culture
409 tube. Outgrowth was at 28°C for 2 h followed by plating on THB agar supplemented with 5 µg/mL
410 erythromycin. Plates were incubated for 48 h at 28°C. A single colony was cultured overnight in
411 5 mL THB with 5 µg/mL erythromycin at 28°C. The culture was screened via PCR for the plasmid
412 insert with the initial denaturing step extended to 10 min. The overnight culture was diluted 1:1000
413 THB containing 5 µg/mL erythromycin and incubated overnight at 37°C to promote single cross
414 over events. The culture was then serial diluted and plated on THB agar plates with antibiotic and

415 incubated at 37°C overnight. Colonies were screened for single crossover events by PCR. Single
416 crossover colonies were inoculated in 5 mL THB at 28°C to promote double crossover events.
417 Overnight cultures were diluted 1:1000 into 5 mL THB containing sterile 0.75 M sucrose and
418 incubated at 37°C. Overnight cultures were serial diluted and plated on THB agar and incubated
419 at 37°C overnight. Colonies were patched onto THB agar with and without 5 µg/mL erythromycin
420 to confirm loss of plasmid. Colonies were also screened by PCR for the loss of *mprF*. Colonies
421 positive for the loss of *mprF* were inoculated into 5 mL THB at 37°C. Cultures were stocked and
422 gDNA extracted as described above, with minor modifications. Sequence confirmation of the
423 *mprF* knockout was done via Sanger sequencing (Massachusetts General Hospital DNA Core or
424 CU Anschutz Molecular Biology Core). The mutant was grown overnight in 15 mL THB at 37°C
425 and pelleted at 6,150 x *g* for 5 min in a Sorvall RC6+ centrifuge at room temperature for lipid
426 extraction as described. Genomic DNA of COH1Δ*mprF* was isolated as described above and
427 whole genome sequencing was performed in paired-end reads (2 by 150 bp) on the Illumina
428 NextSeq 550 platform at the Microbial Genome Sequencing Center (Pittsburgh, PA).

429

430 **Complementation of *mprF* in COH1Δ*mprF* and CJB111Δ*mprF***

431 Electrocompetent COH1Δ*mprF* were generated as previously described (27). Briefly, GBSΔ*mprF*
432 was inoculated into 5 mL THB with 0.6% glycine and grown overnight. The culture was expanded
433 to 50 mL in pre-warmed THB with 0.6% glycine and grown to an OD₆₀₀ nm of 0.3 and pelleted for
434 10 min at 3200 x *g* at 4°C in a Sorvall RC6+ floor centrifuge. The pellet was kept on ice through
435 the remainder of the protocol. The pellet was washed twice with 25 mL and once with 10 mL of
436 cold 0.625 M sucrose and pelleted as above. The cell pellet was resuspended in 400 µL of cold
437 20% glycerol, aliquoted in 50 µL aliquots, and used immediately or stored at -80°C until use.
438 Electroporation was performed as described above, with recovery in THB supplemented with 0.25
439 M sucrose, and plated on THB agar with kanamycin at 300 µg/mL.

440 **Acidic Bligh-Dyer extractions**

441 Centrifugation was performed using a Sorvall RC6+ centrifuge. Cultures were pelleted at 4,280 x
442 g for 5 min at room temperature unless otherwise stated. The supernatants were removed, and
443 cell pellets were stored at -80°C until acidic Bligh-Dyer lipid extractions were performed as
444 described (12). Briefly, cell pellets were resuspended in 1X PBS (Sigma-Aldrich) and transferred
445 to Corning Pyrex glass tubes with PTFE-lined caps (VWR), followed by 1:2 vol:vol
446 chloroform:methanol addition. Single phase extractions were vortexed periodically and incubated
447 at room temperature for 15 minutes before 500 x g centrifugation for 10 min. A two-phase Bligh-
448 Dyer was achieved by addition of 100 µL 37% HCl, 1 mL CHCl₃, and 900 µl of 1X PBS, which
449 was then vortexed and centrifuged for 5 min at 500 x g. The lower phase was removed to a new
450 tube and dried under nitrogen before being stored at -80°C prior to lipidomic analysis.

451

452 **Liquid Chromatography/Electrospray Ionization Mass Spectrometry**

453 Normal phase LC was performed on an Agilent 1200 quaternary LC system equipped with an
454 Ascentis silica HPLC column (5 µm; 25 cm by 2.1 mm; Sigma-Aldrich) as described previously
455 (28, 29). Briefly, mobile phase A consisted of chloroform-methanol-aqueous ammonium
456 hydroxide (800:195:5, vol/vol), mobile phase B consisted of chloroform-methanol-water-aqueous
457 ammonium hydroxide (600:340:50:5, vol/vol), and mobile phase C consisted of chloroform-
458 methanol-water-aqueous ammonium hydroxide (450:450:95:5, vol/vol). The elution program
459 consisted of the following: 100% mobile phase A was held isocratically for 2 min, then linearly
460 increased to 100% mobile phase B over 14 min, and held at 100% mobile phase B for 11 min.
461 The LC gradient was then changed to 100% mobile phase C over 3 min, held at 100% mobile
462 phase C for 3 min, and, finally, returned to 100% mobile phase A over 0.5 min and held at 100%
463 mobile phase A for 5 min. The LC eluent (with a total flow rate of 300 µl/min) was introduced into

464 the ESI source of a high-resolution TripleTOF5600 mass spectrometer (Sciex, Framingham, MA).
465 Instrumental settings for negative-ion ESI and MS/MS analysis of lipid species were: IS = -4,500
466 V, CUR = 20 psi, GSI = 20 psi, DP = -55 V, and FP = -150V. Settings for positive-ion ESI and
467 MS/MS analysis were: IS = +5,000 V, CUR = 20 psi, GSI = 20 psi, DP = +55 V, and FP = +50V.
468 The MS/MS analysis used nitrogen as the collision gas. Data analysis was performed using
469 Analyst TF1.5 software (Sciex, Framingham, MA).

470

471 **pH-adjusted THB growth**

472 Approximately 30 mL of fresh THB were adjusted to different pH values, measured using a Mettler
473 Toledo FiveEasy pH/MV meter, and sterile-filtered using 0.22 μ M syringe filters. A final volume of
474 200 μ L culture medium was aliquoted per well in a flat-bottom 96 well plate (Falcon); culture media
475 were not supplemented with antibiotics. Overnight cultures of GBS strains were used to inoculate
476 the wells to a starting OD_{600nm} 0.02 per well. Plates were incubated for 24 h at 37°C before OD_{600nm}
477 was read using a BioTek MX Synergy 2 plate reader. This experiment was performed in biological
478 triplicate.

479

480 **hCMEC cell adherence and invasion assays**

481 Human Cerebral Microvascular Endothelial cells hCMEC/D3 (obtained from Millipore) were grown
482 in EndoGRO-MV complete media (Millipore, SCME004) supplemented with 5% fetal bovine
483 serum (FBS) and 1 ng/ml fibroblast growth factor-2 (FGF-2; Millipore). Cells were grown in tissue
484 culture treated 24 well plates and 5% CO₂ at 37°C.

485

486 Assays to determine the total number of bacteria adhered to host cells or intracellular bacteria
487 were performed as described previously (15, 16). Briefly, bacteria were grown to mid log phase
488 (OD_{600nm} 0.4-0.5) and normalized to 1×10^8 to infect cell monolayers at a multiplicity of infection
489 (MOI) of 1 (1×10^5 CFU per well). The total cell-associated GBS were recovered after 30 min
490 incubation. Cells were washed slowly five times with 500 μ L 1X PBS (Sigma) and detached by
491 addition of 100 μ L of 0.25% trypsin-EDTA solution (Gibco) and incubation for 5 min before lysing
492 the eukaryotic cells with the addition of 400 μ L of 0.025% Triton X-100 (Sigma) and vigorous
493 pipetting. The lysates were then serially diluted and plated on THB agar and incubated overnight
494 to determine CFU. Bacterial invasion assays were performed as described above except infection
495 plates were incubated for 2 h before incubation with 100 μ g gentamicin (Sigma) and 5 μ g penicillin
496 (Sigma) supplemented media for an additional 2 h to kill all extracellular bacteria, prior to being
497 trypsinized, lysed, and plated as described. Experiments were performed in biological triplicate
498 with four technical replicates per experiment.

499

500 **Murine model of GBS hematogenous meningitis**

501 All animal experiments were conducted under the approval of the Institutional Animal Care and
502 Use Committee (#00316) at the University of Colorado Anschutz Medical Campus and
503 performed using accepted veterinary standards. The murine meningitis model was performed as
504 previously described (16, 30, 31). Briefly, 7-week-old male CD1 (Charles River) mice were
505 challenged intravenously with 1×10^9 CFU of WT COH1 or the isogenic $\Delta mprF$ mutant. At 72 h
506 post-infection, mice were euthanized and blood and brain tissue were harvested, homogenized,
507 and serially diluted on THB agar plates to determine bacterial CFU.

508

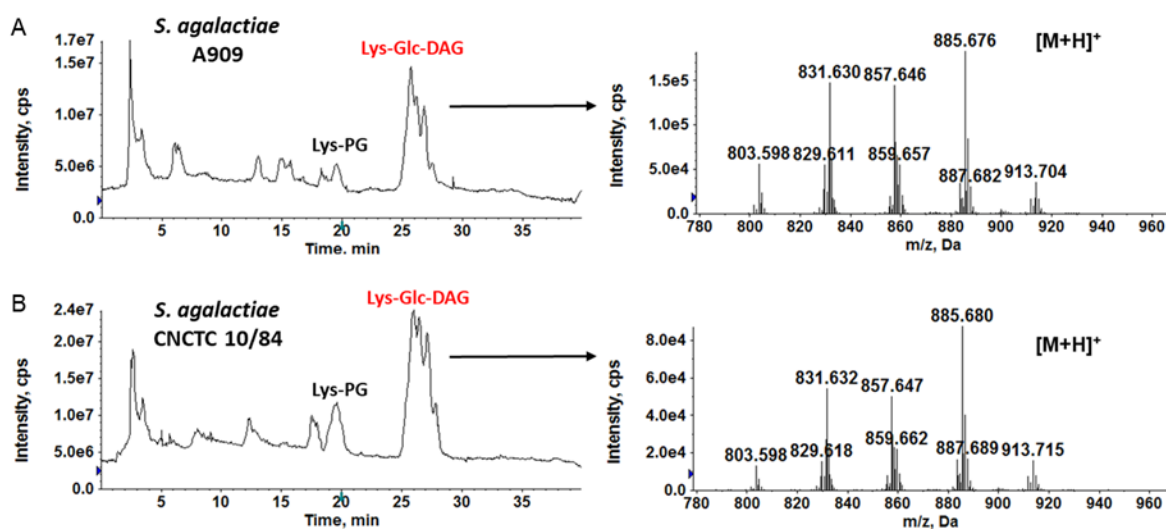
509

510 **Histology and ELISA**

511 Mouse brain tissue was frozen in OCT compound (Sakura) and sectioned using a CM1950
512 cryostat (Leica). Sections were stained using hematoxylin and eosin (Sigma) and images were
513 taken using a BZ-X710 microscope (Keyence). Images were analyzed using ImageJ software.
514 Meningeal thickening was quantified from sections taken from three different mice per group, and
515 six images per slide. Meningeal thickening was quantified across two points per image. KC protein
516 from mouse brain homogenates was detected by enzyme-linked immunosorbent assay according
517 to the manufacturer's instructions (R&D systems).

518

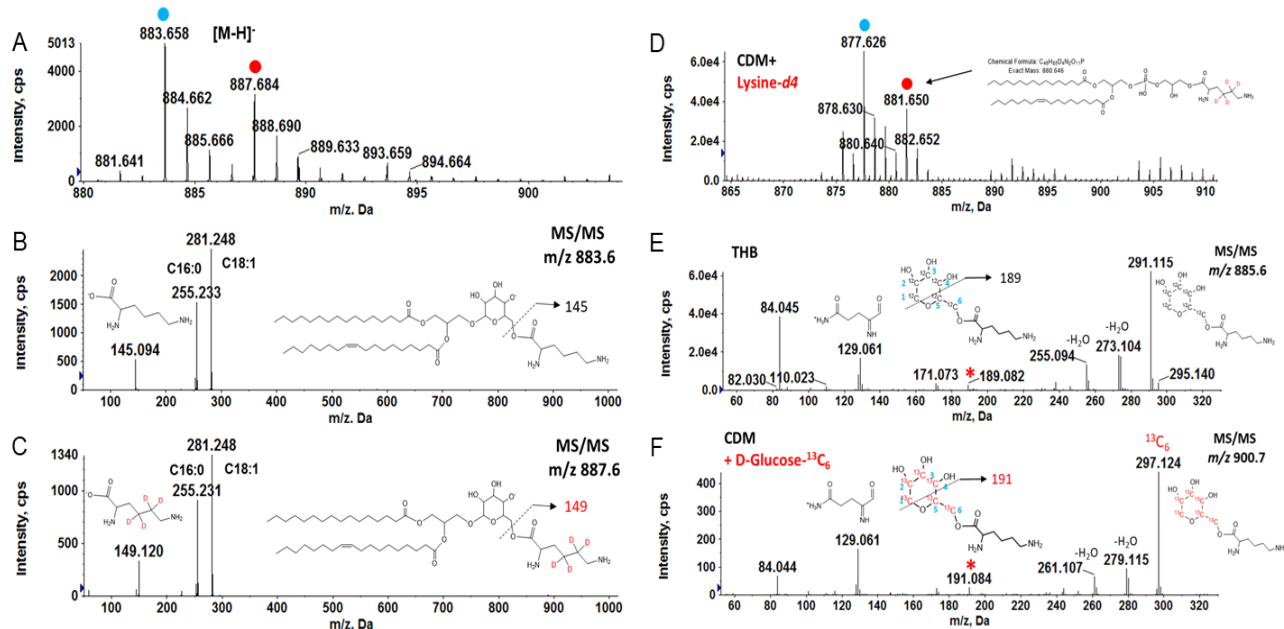
519



520

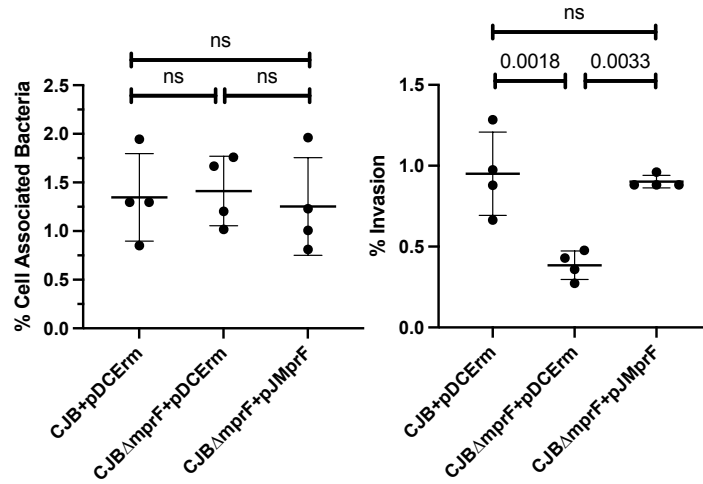
521 **Supplemental Figure S1. Detection of Lys-PG and Lys-Glc-DAG in *S. agalactiae* A909 and**
522 ***S. agalactiae* CNCTC 10/84.** Positive TICs (left panels) showing the presence of Lys-PG and
523 Lys-Glc-DAG in *S. agalactiae* A909 and *S. agalactiae* CNCTC 10/84. Mass spectra (right panels)
524 show the [M+H]⁺ ions of Lys-Glc-DAG.

525



526
 527 **Supplemental Figure S2. Isotopic incorporation of deuterated lysine and ^{13}C -labeled**
 528 **glucose into Lys-Glc-DAG and Lys-PG.** The lipid extracts of *S. agalactiae* COH1 cultured in
 529 DM, DM supplemented with 450 μM L-lysine-*d*4 (4,4,5,5-D4), or in DM containing 0.5% w/v D-
 530 Glucose ($\text{U-}^{13}\text{C}_6$) were analyzed by LC-ESI/MS in the positive ion mode. A) Negative ESI/MS of
 531 $[\text{M-H}]^-$ ions of major Lys-Glc-DAG species in *S. agalactiae* COH1 when cultured in DM
 532 supplemented with lysine-*d*4. The incorporation of lysine-*d*4 into Lys-Glc-DAG is evidenced by an
 533 upward m/z shift of 4 Da of the $[\text{M-H}]^-$ ion (from m/z 883 to m/z 887). B) MS/MS of $[\text{M-H}]^-$ at m/z
 534 883.6 produces a deprotonated lysine residue at m/z 145. C) MS/MS of $[\text{M-H}]^-$ at m/z 887.6
 535 produces a deprotonated lysine-*d*4 residue at m/z 149. D) $[\text{M+H}]^+$ ions of major Lys-PG species
 536 in *S. agalactiae* COH1 cultured in DM supplemented with lysine-*d*4. The incorporation of lysine-
 537 *d*4 in Lys-PG is evidenced by an upward m/z shift of 4 Da from unlabeled Lys-PG (blue dot) to
 538 labeled Lys-PG (red dot). E) MS/MS of 885.6. A major product ion at m/z 291.1 is derived from
 539 glucose-lysine residue. F) MS/MS of m/z 900.7 (containing fifteen ^{13}C atoms). The presence of
 540 m/z 297.1 (with 6 Da shift) is consistent with glucose in Lys-Glc-DAG is replaced with D-Glucose
 541 ($\text{U-}^{13}\text{C}_6$). The other nine ^{13}C atoms are incorporated into the DAG portion of Lys-Glc-DAG.
 542 Furthermore, MS/MS data indicate that lysine is linked to the C6 position of glucose by the
 543 fragmentation schemes for forming m/z 189 ion from the unlabeled Lys-Glc-DAG and m/z 191
 544 from the ^{13}C -labeled Lys-Glc-DAG.

545



546

547 **Supplemental Figure S3. *In vitro* hCMEC adhesion and invasion of CJB111 strains.** *In vitro*
548 assays for adherence and invasion of hCMEC cells indicates *mprF* contributes to invasion but not
549 adherence to brain endothelium. Data indicates the percentage of the initial inoculum that was
550 recovered. Experiments were performed three times with each condition in quadruplicate. Data
551 from one representative experiment is shown, mean and standard deviation indicated. One-Way
552 ANOVA with Tukey's multiple comparisons statistical test was used. P-values indicated; ns, not
553 significant.

554 **Supplemental Table S1. Observed and calculated exact masses of the [M+H]⁺ ions of Lys-**
555 **Glc-DAG molecular species in *S. agalactiae* COH1.**

Lys-Glc-DAG ¹	[M+H] ⁺	
	Observed mass	Exact mass
C28:1	801.575	801.583
C28:0	803.595	803.599
C30:1	829.610	829.615
C30:0	831.624	831.630
C32:2	855.623	855.630
C32:1	857.644	857.646
C34:2	883.657	883.622
C34:1	885.672	885.677
C36:2	911.686	911.693
C36:1	913.703	913.709

556 ¹The numbers before and after colons indicate the total acyl chain carbon atoms and double
557 bonds, respectively.

558 **Supplemental Table S2. Strains and plasmids used in this study.**

Organism	Strain	Description	Ref
<i>S. agalactiae</i>	ATCC BAA-1176 (COH1)	Wild-type <i>S. agalactiae</i> strain, serotype III	(6)
	COH1 Δ <i>mprF</i>	<i>mprF</i> (GBSCOH1_1931) deletion strain	This work
	COH1 Δ <i>mprF</i> (pABG5)	Empty vector control strain	This work
	COH1 Δ <i>mprF</i> (pGBSMprf)	Expresses GBS <i>mprF</i> from P _{prtF} in pABG5 Δ <i>phoZ</i>	This work
	COH1(pABG5)	Empty vector control	This work
	CJB111	Wild-type <i>S. agalactiae</i> strain, serotype V	(17, 18)
	CJB111 Δ <i>mprF</i>	<i>mprF</i> (ID870_10050) deletion strain	This work
	CJB111 Δ <i>mprF</i> (pDCErm)	Empty vector control strain	This work
	CJB111 Δ <i>mprF</i> (pJMprF)	Expresses GBS <i>mprF</i> in pDCErm	This work
	ATCC BAA-1138 (A909)	Wild-type <i>S. agalactiae</i> strain, serotype Ia	(7)
CNCTC 10/84	Wild-type <i>S. agalactiae</i> strain, serotype V. Obtained from Dr. K Patras, UCSD	(8, 32)	
<i>S. mitis</i>	ATCC 49456	Wild-type <i>S. mitis</i> type strain, also known as NCTC 12261	(33)
	ATCC 49456(pABG5)	Empty vector control	This work
	ATCC 49456(pGBSMprF)	Expresses GBS <i>mprF</i> from P _{prtF} in pABG5 Δ <i>phoZ</i>	This work
	ATCC 49456(pEfmMprF1)	Expresses <i>E. faecium mprF1</i> from P _{prtF} in pABG5 Δ <i>phoZ</i>	This work
	ATCC 49456(pEfmMprF2)	Expresses <i>E. faecium mprF1</i> from P _{prtF} in pABG5 Δ <i>phoZ</i>	This work
<i>E. coli</i>	DH5 α	Plasmid cloning host; F ⁻ , ϕ 80 <i>lacZ</i> Δ M15, <i>recA1</i> , <i>endA1</i> , <i>hsdR17</i> , <i>phoA</i> , <i>s</i> _{upE44} , λ^- <i>thi-1</i> , <i>gyrA96</i> , <i>relA1</i>	(34)
	DH5 α (pABG5)	Empty vector control	This work
	MC1061	Plasmid cloning host; F ⁻ , <i>araD139</i> , Δ (<i>araABC-leu</i>)7696, Δ (<i>lac</i>)X74, <i>galU</i> , <i>galK</i> , <i>hsdR2</i> , (<i>r</i> κ^- m κ^+), <i>mcrB1</i> , <i>rpsL</i> , (Str ^r)	(35)
	MC1061(pDCErm)	Empty vector control	This work

DH5 α (pGBSMprF)	Expresses COH1 <i>mprF</i> (GBSCOH1_1931) from P _{prtF} in pABG5 Δ <i>phoZ</i>	This work
DH5 α (pEfmMprF1)	Expresses <i>E. faecium mprF1</i> from P _{prtF} in pABG5 Δ <i>phoZ</i>	This work
DH5 α (pEfmMprF2)	Expresses <i>E. faecium mprF1</i> from P _{prtF} in pABG5 Δ <i>phoZ</i>	This work
DH5 α (pMBMprFKO)	Allelic exchange plasmid containing ~2 kb sequence flanking GBSCOH1_1931	This work
MC1061(pJMprFKO)	Allelic exchange plasmid containing ~2 kb sequence flanking ID870_10050	This work
MC1061(pJMprF)	Expresses CJB11 <i>mprF</i> from P _{tetM/erm} in pDCErm	This work
<i>E. faecium</i>	1,231,410	Wild type <i>E. faecium</i> strain (36)
Plasmid	Description	Ref
pABG5 Δ <i>phoZ</i>	Constitutive expression vector for streptococci with the P _{prtF} promoter. Confers kanamycin resistance. Referred to as pABG5 throughout the text	(23)
pGBSMprF	pABG5 Δ <i>phoZ</i> expressing COH1 <i>mprF</i> (GBSCOH1_1931) from P _{prtF}	This work
pEfmMprF1	pABG5 Δ <i>phoZ</i> expressing <i>E. faecium</i> 1,231,410 <i>mprF1</i> (EFTG_00601) from P _{prtF}	This work
pMBSacB	Allelic exchange plasmid for <i>S. agalactiae</i> . Confers erythromycin resistance and sucrose sensitivity	(25)
pMBMprFKO	Knockout plasmid containing ~2 kb sequence flanking GBSCOH1_1931	This work
pJMprFKO	Knockout plasmid containing ~2 kb sequence flanking ID870_10050	This work
pDCErm	Constitutive expression vector for streptococcus from P _{tetM/erm}	(24)
pJMprF	pDCErm expressing CJB111 <i>mprF</i> (ID870_10050)	This work

559

560

561 **Supplemental Table S3. Primers used in this study.**

Primer	5' – 3' sequence	Use
GBS_MprF_F	GAGAGGTCCTTTCC TTGAAAAAGC TAATTGAAAAAGTC	Amplify GBSCOH1_1931 for Gibson assembly
GBS_MprF_R	ACCAATACCTTTATC TTTATTTAACAA TCTTAATTTTACTATC	Amplify GBSCOH1_1931 for Gibson assembly
Faec_MprF1_F	GAGAGGTCCTTTCC TTGTTAAAAA ATACCATACAATG	Amplify EFTG_00601 for Gibson assembly
Faec_MprF1_R	ACCAATACCTTTATC TTAATACTTTC TTCGTATCC	Amplify EFTG_00601 for Gibson assembly
MpF_SacII	ACGTCA CCGCGG TTGAAAAAGCTAA TTGAAAAAGTC	Amplify CJB111 <i>mprF</i> ID870_10050 for ligation
MpR_BamHI	ACGTCA GGATCC TTTATTTAACAACTCT TAATTTTACTATC	Amplify CJB111 <i>mprF</i> ID870_10050 for ligation
pABG5-5'	GGAAAGGGACCTCTCTCCTAAAC	Linearize pABG5Δ <i>phoZ</i> for Gibson assembly
pABG5-3'	GATAAAGGTATTGGTAAATAACAAA	Linearize pABG5Δ <i>phoZ</i> for Gibson assembly
Expression plasmid sequencing		
GBS_S1	GAATGGAATAATATAGTAGGCT	For sequencing pGBSMprF/pJMprF, amplifies with pABG5_Fup2/ pF
GBS_S2	GATTGTATCCCTTATTCC	For sequencing pGBSMprF/pJMprF, amplifies with GBS_S3
GBS_S3	CGATTCAATAGCTTCAC	For sequencing pGBSMprF/pJMprF, amplifies with GBS_S2
GBS_S4	GATAAAAGGCTCTACTGG	For sequencing pGBSMprF/pJMprF, amplifies with pABG5_FDwn/pR
pABG5_FDwn	CCAATAATAATGACTAGAGAAG	For pABG5 plasmid insert sequencing
pABG5_Fup2	CAAAGGTTTCGACTTTTCACC	For pABG5 plasmid insert sequencing
EF1_S1	GAATAACGCTGATCAAAAAGT	For sequencing pEfmMprF1, amplifies with pABG5_Fup2
EF1_S2	TGCCAAGAGAAATAGTC	For sequencing pEfmMprF1, amplifies with EF1_S3
EF1_S3	ACAATCTCTTCGCTTG	For sequencing pEfmMprF1, amplifies with EF1_S2
EF1_S4	CCAACTGTTCTTCTCCAA	For sequencing pEfmMprF1, amplifies with pABG5_FDwn
pF	AGCGCTAGGAGGAAAC	For pDCerm plasmid insert sequencing
pR	CCCATGCCATCTCCAATC	For pDCerm plasmid insert sequencing
GBSCOH1_1931 knockout plasmid construction, sequencing, and integration screening		
Mp1F_PstI	ACGTCACTGCAG TCAATTAGCTTTT TCAACAATTC	Amplifies upstream fragment from within GBSCOH1_1931/ID870_10050 leaving 6 codons, with Mp1R_XhoI
Mp1R_XhoI	ACGTCACTCGAG GCTGTTTATGGTG CTTTG	5' most primer of upstream fragment, amplifies with Mp1F_PstI
Mp2F_XbaI	ACGTCA TCTAGAGAAAAGGCTAGAT TACGAAC	3' most primer of downstream fragment, amplifies with Mp2R_PstI
Mp2R_PstI	ACGTCACTGCAG GTTAAATAAGCTTT ATTTGGCA	Amplifies downstream fragment leaving 2 codons and stop codon of GBSCOH1_1931/ID870_10050, with Mp2F_XbaI
T7 promoter	TAATACGACTCACTATAGGG	Amplifies with MpS5F below to sequence plasmid, amplifies with T3 promoter for insert screening and plasmid presence
T3 promoter	AATTAACCCTCACTAAAGGG	Amplifies with MpS3R below, amplifies with T7 promoter for insert screening and plasmid presence
Int_F	GCTAATTGAACTGCAGGTTAAATAA G	Anneals at <i>mprF</i> knockout site, amplifies with Out_R for single integration screening

Out_R	GCTATTATATTTAGTGGTTTAATTGG	Anneals outside recombination arms, amplifies with Int_F, for single integration screening
-------	----------------------------	--

Genomic knockout region sequencing

MpS3F	CATTAGCTAGTCTTATCGGAG	Anneals outside integration arms, amplifies with MpS3R
MpS3R	ACAGCTACTTGGTAGTTCA	Amplifies with MpS3F
MpS4F	GCTACTAAGGCAAGATACG	Amplifies with MpS4R, knockout screening and plasmid sequencing primer
MpS4R	ATGGTCAGCGATGGTG	Amplifies with MpS4F, knockout screening and plasmid sequencing primer
MpS5F	CATAAGCGAAATAACTTGAG	Amplifies with MpS5R
MpS5R	GTATACAACGGCTTGATTGG	Anneals outside integration arms, amplifies with MpS5F

562

563

564 **References**

- 565 1. Wilkinson HW. 1978. Group B Streptococcal Infection in Humans. Annual Review
566 of Microbiology 32:41-57.
- 567 2. Doran KS, Nizet V. 2004. Molecular pathogenesis of neonatal Group B
568 Streptococcal infection: No longer in its infancy. Molecular Microbiology 54:23-
569 31.
- 570 3. Hall J, Adams NH, Bartlett L, Seale AC, Lamagni T, Bianchi-Jassir F, Lawn JE,
571 Baker CJ, Cutland C, Heath PT, Ip M, Le Doare K, Madhi SA, Rubens CE, Saha
572 SK, Schrag S, Sobanjo-Ter Meulen A, Vekemans J, Gravett MG. 2017. Maternal
573 Disease With Group B *Streptococcus* and Serotype Distribution Worldwide:
574 Systematic Review and Meta-analyses. Clinical infectious diseases : an official
575 publication of the Infectious Diseases Society of America 65:S112-S124.
- 576 4. Schuchat A. 1998. Epidemiology of Group B Streptococcal disease in the United
577 States: shifting paradigms. Clinical Microbiology Reviews 11:497-513.
- 578 5. Edwards MS, Rench MA, Haffar AA, Murphy MA, Desmond MM, Baker CJ. 1985.
579 Long-term sequelae of Group B Streptococcal meningitis in infants. The Journal
580 of Pediatrics 106:717-22.
- 581 6. Kuypers JM, Heggen LM, Rubens CE. 1989. Molecular analysis of a region of
582 the Group B *Streptococcus* chromosome involved in type III capsule expression.
583 Infection and Immunity 57:3058-65.
- 584 7. Lancefield RC, McCarty M, Everly WN. 1975. Multiple mouse-protective
585 antibodies directed against Group B Streptococci. Special reference to antibodies
586 effective against protein antigens. The Journal of Experimental Medicine
587 142:165-79.
- 588 8. Wilkinson HW. 1977. Nontypable Group B Streptococci isolated from human
589 sources. Journal of Clinical Microbiology 6:183-4.
- 590 9. Doran KS, Engelson EJ, Khosravi A, Maisey HC, Fedtke I, Equils O, Michelsen
591 KS, Arditi M, Peschel A, Nizet V. 2005. Blood-brain barrier invasion by Group B
592 *Streptococcus* depends upon proper cell-surface anchoring of lipoteichoic acid.
593 The Journal of Clinical Investigation 115:2499-507.
- 594 10. Peschel A, Jack RW, Otto M, Collins LV, Staubitz P, Nicholson G, Kalbacher H,
595 Nieuwenhuizen WF, Jung G, Tarkowski A, Van Kessel KPM, Van Strijp JAG.
596 2001. *Staphylococcus aureus* resistance to human defensins and evasion of
597 neutrophil killing via the novel virulence factor MprF is based on modification of
598 membrane lipids with L-lysine. Journal of Experimental Medicine 193:1067-1076.
- 599 11. Roy H, Ibba M. 2008. RNA-dependent lipid remodeling by bacterial multiple
600 peptide resistance factors. Proceedings of the National Academy of Sciences of
601 the United States of America 105:4667-4672.
- 602 12. Joyce LR, Guan Z, Palmer KL. 2019. Phosphatidylcholine Biosynthesis in *Mitis*
603 Group Streptococci via Host Metabolite Scavenging. Journal of Bacteriology
604 201:e00495-19.
- 605 13. Adams HM, Joyce LR, Guan Z, Akins RL, Palmer KL. 2017. *Streptococcus mitis*
606 and *S. oralis* Lack a Requirement for CdsA, the Enzyme Required for Synthesis
607 of Major Membrane Phospholipids in Bacteria. Antimicrobial Agents and
608 Chemotherapy 61:e02552-16.

- 609 14. Roy H. 2009. Tuning the properties of the bacterial membrane with
610 aminoacylated phosphatidylglycerol. *IUBMB Life* 61:940-953.
- 611 15. Deng L, Spencer BL, Holmes JA, Mu R, Rego S, Weston TA, Hu Y, Sanches GF,
612 Yoon S, Park N, Nagao PE, Jenkinson HF, Thornton JA, Seo KS, Nobbs AH,
613 Doran KS. 2019. The Group B Streptococcal surface antigen I/II protein, BspC,
614 interacts with host vimentin to promote adherence to brain endothelium and
615 inflammation during the pathogenesis of meningitis. *PLoS pathogens*
616 15:e1007848.
- 617 16. Spencer BL, Deng L, Patras KA, Burcham ZM, Sanches GF, Nagao PE, Doran
618 KS. 2019. Cas9 contributes to Group B Streptococcal colonization and disease.
619 *Frontiers in Microbiology* 10:1-15.
- 620 17. Faralla C, Metruccio MM, De Chiara M, Mu R, Patras KA, Muzzi A, Grandi G,
621 Margarit I, Doran KS, Janulczyk R. 2014. Analysis of two-component systems in
622 group B Streptococcus shows that RgfAC and the novel FspSR modulate
623 virulence and bacterial fitness. *mBio* 5:e00870-14.
- 624 18. Spencer BL, Chatterjee A, Duerkop BA, Baker CJ, Doran KS. 2021. Complete
625 Genome Sequence of Neonatal Clinical Group B Streptococcal Isolate CJB111.
626 *Microbiology resource announcements* 10.
- 627 19. Mu R, Cutting AS, Del Rosario Y, Villarino N, Stewart L, Weston TA, Patras KA,
628 Doran KS. 2016. Identification of CiaR Regulated Genes That Promote Group B
629 Streptococcal Virulence and Interaction with Brain Endothelial Cells. *PLoS One*
630 11:e0153891.
- 631 20. Van De Rijn I, Kessler RE. 1980. Growth characteristics of Group A Streptococci
632 in a new chemically defined medium. *Infection and Immunity* 27:444-448.
- 633 21. Chang JC, LaSarre B, Jimenez JC, Aggarwal C, Federle MJ. 2011. Two Group A
634 Streptococcal peptide pheromones act through opposing rgg regulators to control
635 biofilm development. *PLoS Pathogens* 7:e1002190.
- 636 22. Gupta R, Shah P, Swiatlo E. 2009. Differential gene expression in *Streptococcus*
637 *pneumoniae* in response to various iron sources. *Microbial Pathogenesis* 47:101-
638 109.
- 639 23. Granok AB, Parsonage D, Ross RP, Caparon MG. 2000. The RofA binding site
640 in *Streptococcus pyogenes* is utilized in multiple transcriptional pathways.
641 *Journal of bacteriology* 182:1529-40.
- 642 24. Jeng A, Sakota V, Li Z, Datta V, Beall B, Nizet V. 2003. Molecular genetic
643 analysis of a group A *Streptococcus* operon encoding serum opacity factor and a
644 novel fibronectin-binding protein, SfbX. *J Bacteriol* 185:1208-17.
- 645 25. Hooven TA, Bonakdar M, Chamby AB, Ratner AJ. 2019. A Counterselectable
646 Sucrose Sensitivity Marker Permits Efficient and Flexible Mutagenesis in
647 *Streptococcus agalactiae*. *Applied and Environmental Microbiology* 85:1-13.
- 648 26. Holo H, Nes IF. 1989. High-frequency transformation, by electroporation, of
649 *Lactococcus lactis* subsp. *cremoris* grown with glycine in osmotically stabilized
650 media. *Applied and Environmental Microbiology* 55:3119-3123.
- 651 27. Framson PE, Nittayajarn A, Merry J, Youngman P, Rubens CE. 1997. New
652 genetic techniques for Group B Streptococci: High-efficiency transformation,
653 maintenance of temperature-sensitive pWV01 plasmids, and mutagenesis with
654 Tn917. *Applied and Environmental Microbiology* 63:3539-3547.

- 655 28. Tan BK, Bogdanov M, Zhao J, Dowhan W, Raetz CRH, Guan Z. 2012. Discovery
656 of a cardiolipin synthase utilizing phosphatidylethanolamine and
657 phosphatidylglycerol as substrates. *Proceedings of the National Academy of*
658 *Sciences* 109:16504-16509.
- 659 29. Li C, Tan BK, Zhao J, Guan Z. 2016. In vivo and in vitro synthesis of
660 phosphatidylglycerol by an *Escherichia coli* cardiolipin synthase. *Journal of*
661 *Biological Chemistry* 291:25144-25153.
- 662 30. Kim BJ, Hancock BM, Bermudez A, Del Cid N, Reyes E, van Sorge NM, Lauth X,
663 Smurthwaite CA, Hilton BJ, Stotland A, Banerjee A, Buchanan J, Wolkowicz R,
664 Traver D, Doran KS. 2015. Bacterial induction of Snail1 contributes to blood-
665 brain barrier disruption. *The Journal of Clinical Investigation* 125:2473-83.
- 666 31. Banerjee A, Kim BJ, Carmona EM, Cutting AS, Gurney MA, Carlos C, Feuer R,
667 Prasadarao NV, Doran KS. 2011. Bacterial Pili exploit integrin machinery to
668 promote immune activation and efficient blood-brain barrier penetration. *Nature*
669 *Communications* 2:462.
- 670 32. Hooven TA, Randis TM, Daugherty SC, Narechania A, Planet PJ, Tettelin H,
671 Ratner AJ. 2014. Complete Genome Sequence of *Streptococcus agalactiae*
672 CNCTC 10/84, a Hypervirulent Sequence Type 26 Strain. *Genome*
673 *Announcements* 2:e01338-14.
- 674 33. Kilian M, Mikkelsen L, Henrichsen J. 1989. Taxonomic Study of Viridans
675 Streptococci: Description of *Streptococcus gordonii* sp. nov. and Emended
676 Descriptions of *Streptococcus sanguis* (White and Niven 1946), *Streptococcus*
677 *oralis* (Bridge and Sneath 1982), and *Streptococcus mitis* (Andrewes and Horder
678 1906). *International Journal of Systematic Bacteriology* 39:471-484.
- 679 34. Taylor RG, Walker DC, McInnes RR. 1993. *E. coli* host strains significantly affect
680 the quality of small scale plasmid DNA preparations used for sequencing. *Nucleic*
681 *Acids Research* 21:1677-1678.
- 682 35. Casadaban MJ, Cohen SN. 1980. Analysis of gene control signals by DNA fusion
683 and cloning in *Escherichia coli*. *J Mol Biol* 138:179-207.
- 684 36. Palmer KL, Carniol K, Manson JM, Heiman D, Shea T, Young S, Zeng Q, Gevers
685 D, Feldgarden M, Birren B, Gilmore MS. 2010. High-quality draft genome
686 sequences of 28 *Enterococcus* sp. isolates. *Journal of Bacteriology* 192:2469-70.

687

688